8 Lidars and wind turbine control

David Schlipf, Oliver Bischoff, Martin Hofsäß,
Andreas Rettenmeier, Juan José Trujillo, and Martin Kühn
Endowed Chair of Wind Energy, Institute of Aircraft Design,
Universität Stuttgart, Stuttgart, Germany

8.1 Introduction

Reducing mechanical loads caused by atmospheric turbulence and energy optimization in the presence of varying wind are the key issue for wind turbine control. In terms of control theory changes in the inflowing wind field as gusts, varying shears and directional changes represent unknown disturbances. However, conventional feedback controllers can compensate such excitations only with a delay since the disturbance has to be detected by its effects to the turbine. This usually results in undesired loads and energy losses of wind turbines.

From the control theory point of view disturbance rejection can be improved by a feed-forward control if the disturbance is known. Not fully covered by theory, but used in practice is the further advantage of knowing the disturbance in the future, e.g. in chassis suspension or in daily life when vision is used to circumnavigate obstacles with a bicycle.

In a similar way wind field measurements with remote sensing technologies such as lidar might pave the way for predictive wind turbine control strategies aiming to increase energy yield and reduce excessive loads on turbine components. Remote sensing offers wind speed tracking at various points in space and time in advance of reaching the turbine and before hitting sensors at the blades or nacelle. This provides the control and safety system with sufficient reaction and processing time.

In Figure 75 the different steps for predictive wind turbine control are shown. The objective of the first step is to obtain wind fields in different distances in front of the turbine, e.g. by use of lidar. In the next step, turbulence theory, e.g. the "Taylor's frozen turbulence theorem", is considered when modelling the wind on its way towards the turbine. In the last step, the predicted future wind fields are used to improve wind turbine control by model predictive control strategies.

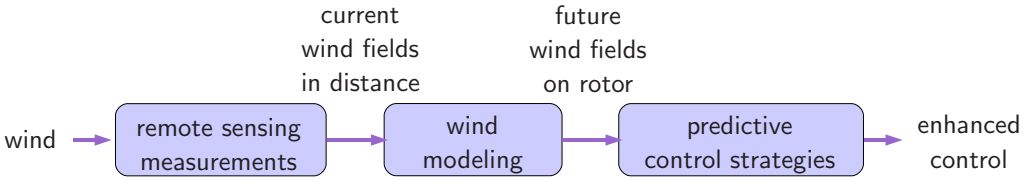

Figure 75: Steps in model predictive wind turbine control assisted by remote sensing

8.2 Measuring wind fields with lidar

Wind fields can be considered as time variant vector fields: one vector **a** in each point in space **p**. Therefore the objective of wind fields assessment is to reconstruct wind fields in discrete space and time points as much as possible.

Commercial lidar systems have the disadvantage that they are not flexible due to measurement in conical domain and normally they are ground based and don't measure in main wind direction. Thus nacelle based lidar systems with scanner or beam splitter are better suited,

but still some issues have to be considered:

- Which points have to be scanned to get best information for control purpose?
- How does the probe volume effect the measurements?
- How can 3D vectors be reconstructed from line-of-sight measurements to obtain information for control? (see section 8.2)

To investigate these effects, a lidar simulator is presented in section 8.2.

The "Cyclops" dilemma

As a Cyclops cannot see three-dimensionally with only one eye, it isn't possible to measure a 3D wind vector with only one lidar system. Three lidar systems focusing in the same point with linearly independent laser beams are needed. With one nacelle mounted lidar system, the two missing systems can be substituted by different assumptions, e.g.:

1. no vertical and no horizontal wind component, or
2. no vertical component and homogenous flow on each height

In Figure 76 the effect of both assumption possibilities is shown. In this case the 3D vectors in p_1 and p_2 (measured in the same height) should be reconstructed from the line-of-sight wind speeds v_{los1} and v_{los2}. The first assumption yield a_{11} and a_{21} representing a horizontal shear. With the second assumption the resulting vectors a_{21} and a_{22} are equal representing a cross-flow, as homogenous flow on each height was assumed.

The dilemma consist, if the lidar measurement should be used for yaw and pitch control at the same time: If the first assumption is used to calculate the inhomogeneous inflow, perfect alignment is assumed. If the second assumption is used to obtain the misalignment, homogeneous flow is assumed.

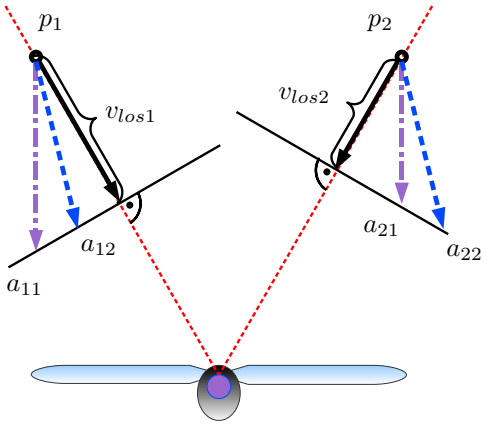

Figure 76: Different possibilities of 3D wind vector reconstruction

WITLIS (WInd Turbine LIdar Simulator)

To understand better the above mentioned effects and to plan measurement campaigns it is helpful to simulate lidar measurements. The main objective of the simulation tool is to reproduce the operation of a nacelle-mounted lidar system. Thus the tool facilitates the evaluation of scanning patterns to find the best hardware and software solution for applications like control, power curve assessment and wake measurements. Wind turbine control strategies based on lidar can be tested with aeroelastic wind turbine simulation tools in a realistic setup.

A modular setup provides software parts that can be used to process measurement data in the same way as simulated data (see Figure 77).

Figure 78 depicts the wind field reconstruction of a simulated measurement: On the left side a generic wind field from TurbSim (Jonkman, 2009) is shown superposed with a wake for better illustration. On the right side the interpolated wind field with WITLIS can be seen. The dots represent a real trajectory as can be done by the adapted Windcube lidar and perfect alignment is assumed. It can be seen that main characteristics can be measured.

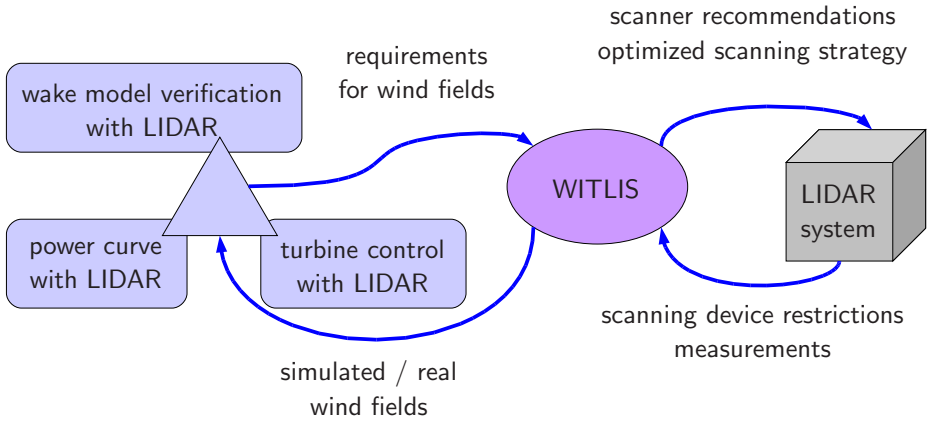

Figure 77: Interactions between the applications, the simulator and the lidar system

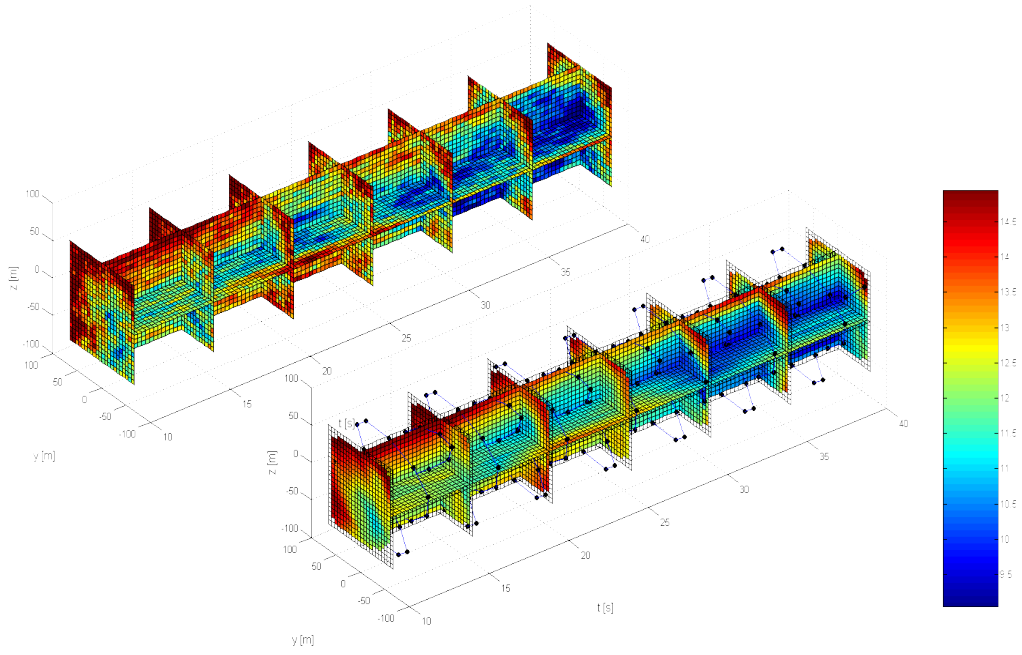

Figure 78: Simulation of realistic lidar measurements in a turbine wake: Original downflow wind component (left) and scanned (right) downflow wind component

8.3 Prediction of wind fields

The inflow wind field for control purpose shouldn't be measured in the rotor plane because of several reasons:

- Because of stability and performance reasons the undisturbed wind field should be measured. But wind in rotor plane is affected by the turbine itself.
- It is difficult to perform measurements in the rotor plane, e.g. with pitot tubes or lidar on the blades.
- Measuring in front of the turbine provides the control system more time to react. The easiest way to model the wind on its way towards the turbine is to use "Taylor's frozen turbulence theorem". It assumes that wind characteristics remain the same while being transported through space with the mean wind speed.

8.4 Improving control

The new information of upwind wind speeds obtained by lidar measurements can be used for improving the turbines control systems. Thereby we distinguish between four different control activities: Yaw control, speed control, collective pitch control and individual pitch control. Possible benefit and potential is listed respectively in table 13.

Table 13: Possible application and benefit of lidar based control. Here is assumed that measurements are at least as beneficial as (e)stimation.

	benefit	potential	reference
yaw	more energy	up to 12%	Cath the Wind (2009)
speed	more energy	up to 10%(e)	Boukhezzar and Siguerdidjane (2005)
collective pitch	less loads	up to 20%	Schlipf and Kühn (2008)
individual pitch	less loads	up to 30%(e)	Selvam et al. (2009)

In this paper we will focus on advanced collective pitch control only.

Predictive Disturbance Compensation (PDC)

Fluctuating wind speed causes the speed of rotation to vary, which affects the loads to the turbine. The objective of pitch control in full operating load range is therefore to maintain a constant rotational speed of the rotor. The wind speed data provided by a lidar can be used to compensate wind speed fluctuations. The block diagram in figure 79 illustrates the control schema.

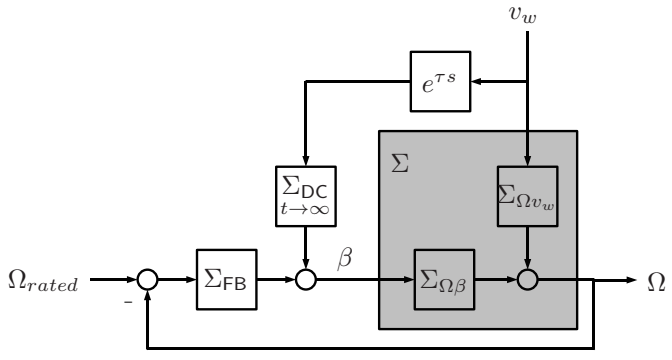

Figure 79: Control loop with predictive disturbance compensation.

The output y (in this case the rotor speed Ω) is influenced by two signals: pitch angle β which is identically equal to the control input u and the effective wind speed v_{eff} which is a disturbance d in terms of control theory. Subsequently the wind turbine system Σ can theoretically be divided into two subsystems, Σ_{yu} and Σ_{yd}. If d is now forwarded by a transfer function Σ_{DC} to the control input u, a compensation of the disturbance can be reached. In this case the feedback controller Σ_{FB} is responsible for reference signal tracking and Σ_{DC} for disturbance rejection.

$\Sigma_{\text{DC}} = -\Sigma_{yu}^{-1}\Sigma_{yd}$ would give a perfect compensation, but in practice the inversion of the nonlinear dynamic turbine model Σ_{yu} cannot be calculated. Therefore a static compensation is proposed

$$\underset{t\to\infty}{\Sigma_{\text{DC}}} = u_{\text{ss}}(d_{\text{ss}})$$

which is the static value u_{ss} of the system input subject to the static disturbance d_{ss}. The feedback controller Σ_{FB} then will react during the dynamic transitions.

The time interval of the transition is influenced by the difference in the dynamic orders of Σ_{yd} and Σ_{yu}. In the case of pitch control Σ_{yu} has a higher dynamic order, because pitch angles have a delayed impact on the rotor speed compared to the wind disturbance. Therefore a prediction time τ shifts the disturbance signal in time in the way that the pitch moves earlier. Due to the lidar measurement in front of the rotor plane this prediction is possible.

Stability of the control loop is influenced neither by the added static feed-forward control nor by time shift, because none of the newly implemented blocks is part of the closed control loop and no new poles were introduced.

Simulation

For evaluation of the proposed controller a Simulink implementation of the generic aeroelastic NREL offshore 5-MW baseline wind turbine model (Jonkman et al., 2009) was used (see Table 14).

Table 14: Specification of the generic NREL wind turbine model.

Rotor	upwind, 3 blades
Rated power output	$P_{\text{rated}} = 5$ MW @ $\Omega_{\text{rated}} = 12.1$ rpm
Dimensions	$D = 126$ m, $h = 90$ m
Controller	collective pitch with gain scheduling
Pitch actuator	2^{nd} order
Filter	$\Omega,\ \beta,\ v_{\text{w}}$: 1^{st} order

For the PDC implementation the shift time τ is chosen to

$$\tau = T_{63,\text{ filter wind}} + T_{63,\text{ pitch actuator}} = 1 \text{ s}$$

where T_{63} denotes the rise time to 63 % of the filters and actuators final value respectively.

The static pitch over wind speed donated $\beta_{\text{ss}}(v_{w,\text{ss}})$ is given in Jonkman et al. (2009) and shown in Figure 80.

The wind is modeled using the stochastic, full-field, turbulent-wind simulator TurbSim (Jonkman, 2009). The measuring of the full-field wind is simulated using WITLIS, see section 8.2. In order to use the wind data for collective pitch control, it is necessary to reduce it to one effective wind speed v_{eff}. Therefore a weighting function (Figure 81) has been developed Schlipf and Kühn (2008). It takes account of the impact of the wind on the aerodynamic torque with respect to the radius using Prandtl root and tip losses.

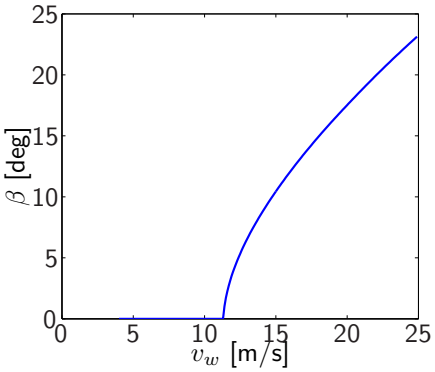

Figure 80: Static pitch over wind speed of the NREL turbine model.

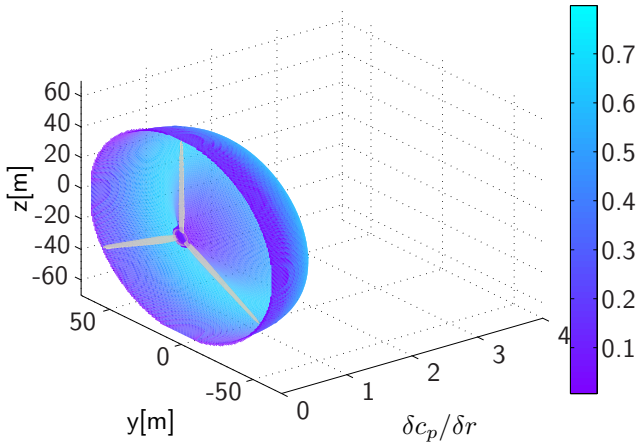

Figure 81: Weighting function for the calculation of the effective wind speed.

Results

The following simulation results show the impact of the proportional-integral (PI) controller and the PDC on rotor speed and bending moment respectively. In frequency domain for PDC a better disturbance rejection in the frequency range up to 0.3 Hz can be observed (figure 82), in which according to the Kaimal spectrum the wind contains most of its energy.

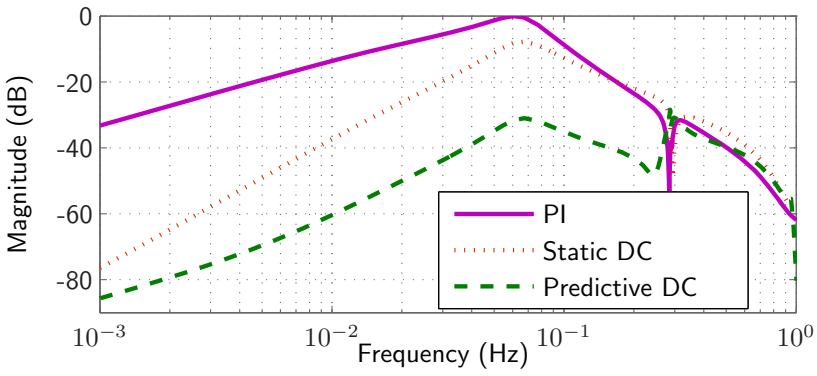

Figure 82: Frequency domain: disturbance rejection of different control strategies.

Extreme Operating Gust (EOG)

Figure 83 shows the results in time domain of simulations of an EOG according to IEC (2005) applied on the NREL wind turbine model. Here, no turbulence occurs and perfect measurement is assumed.

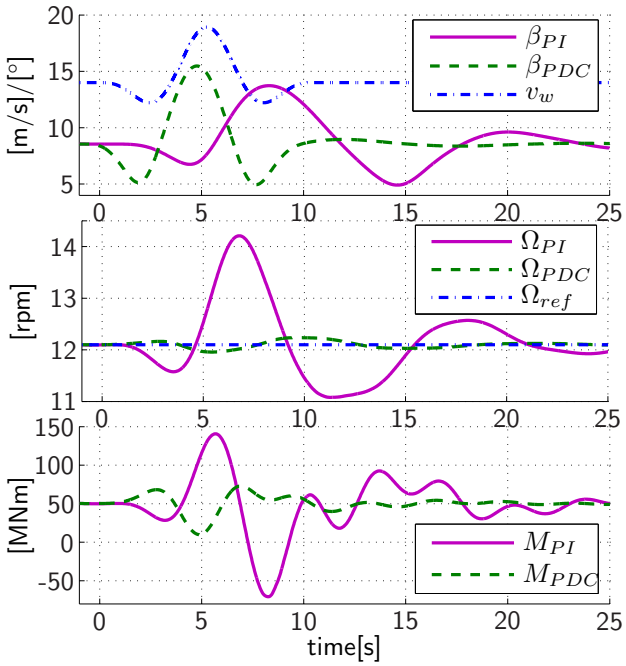

Figure 83: Comparison of conventional and PDC control strategy (EOG). The subscript ref denotes reference

PDC control technique leads to a significantly reduced rotor overspeed. Consequently the fore-aft bending moment M_{yT} at the tower base is decreased by PDC as well, compare table 15.

Table 15: Standard deviation of signals from figure 83

	PI	PDC	PDC/PI
$\sigma(\Omega)$ / [rpm]	0.74	0.08	9%
$\sigma(M_{\mathrm{yT}})$ / [MNm]	38.2	11.0	29%

Turbulent Wind Field

Figure 84 and table 16 show the results for simulations with realistic turbulent wind fields with a spatial resolution of 9 m and a time resolution of 0.05 s. It is based on a Kaimal spectrum with a mean wind speed at hub height of $v_{\mathrm{H}} = 18$ m s^{-1} and turbulence intensity of $TI = 16$ %. Again, perfect measurement is assumed.

Table 16: Standard deviation of signals from figure 84

	PI	PDC	PDC/PI
$\sigma(\Omega)$ / [rpm]	0.42	0.09	21%
$\sigma(M_{\mathrm{yT}})$ / [MNm]	12.8	8.72	68%
$\sigma(\dot{\beta})$ / [deg/s]	0.60	0.47	78%

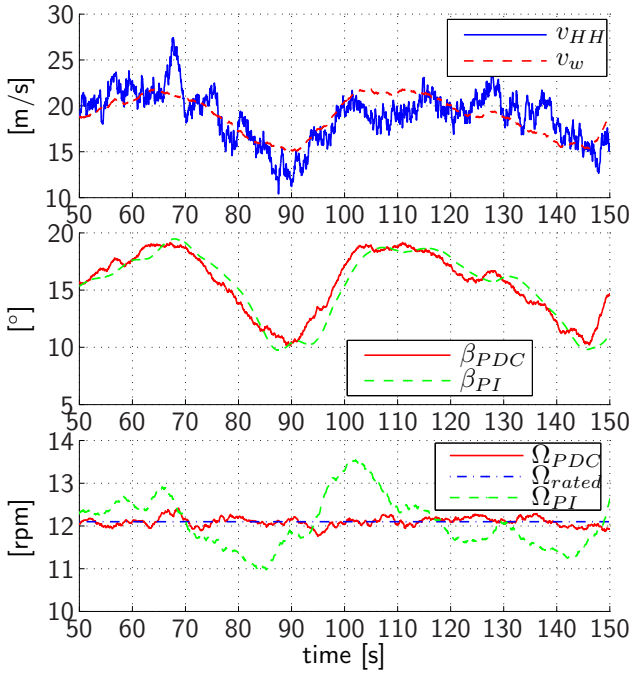

Figure 84: Comparison of conventional and PDC control strategy (turbulent wind field). v_{HH} is the hub height wind speed

PDC reduces rotor speed variation and loads at the tower base despite lower pitch dynamics occur. Simulations also show reduced loads at the blades.

Measurement simulation using WITLIS

In a third simulation the influence of a non-perfect measurement, simulated by WITLIS (see section 8.2) was investigated. From table 17 it can be seen that there is still a remarkable improvement using PDC.

Table 17: Standard deviation of signals from simulation including WITLIS.

	PI	PDC	PDC/PI
$\sigma(\Omega)$ / [rpm]	0.48	0.17	35%
$\sigma(M_{\mathrm{yT}})$ / [MNm]	15.1	11.8	87%
$\sigma(\dot{\beta})$ / [deg/s]	0.79	0.65	83%

Robustness

A weaker performance of the PDC than the conventional PI controller is possible, if there are errors which are not included in the simulation, e.g.

- inaccurate measurements of the wind speed
- wrong calculation of the effective wind speed
- incorrect static pitch curve
- errors in the model used
- invalidity of Taylor's frozen turbulence theorem
- wrong estimate of the shift time τ

Simulations with a varying parameter τ (figure 85) result in a wide range, where the performance results of the PDC remain superior to the PI control.

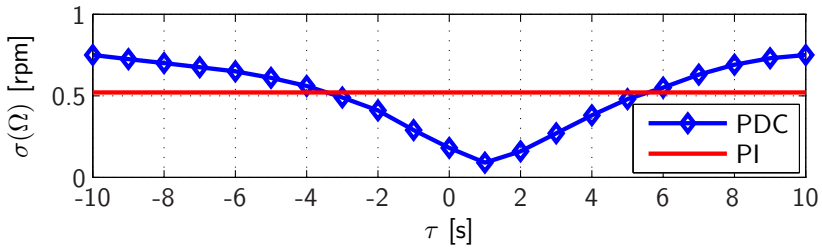

Figure 85: Standard deviation of Ω subject to different prediction time shifts τ for PDC and PI control

Conclusions PDC

The proposed predictive disturbance compensation was presented as a new and powerful control strategy for wind turbine control in full load range. PDC has a guaranteed stability and implementation needs static pitch over wind speed information and one prediction time parameter only.

The performed simulations indicate a significant decrease in rotor speed variation and tower and blade loads without higher pitch actuator activity.

Further research concerns the other control objectives of table 13 as yaw control, speed control and individual pitch control by use of lidar measurements.

Notation

a	horizontal shear of the flow
a	wind vector
d	disturbance
D	rotor diameter
EOG	extreme operating gust
h	hub height
M_{yT}	tower fore-aft bending moment
p	vector point in space
P_{rated}	rated power output
PDC	predictive disturbance compensation
PI	proportional-integral (controller)
T_{X}	X% rising time
TI	turbulence intensity
u	control input
v_{eff}	effective wind speed
v_{HH}	hub height wind speed
v_{los}	line-of-sight wind speed
WITLIS	wind turbine lidar simulator
x_{SS}	steady state of variable x
y	system output
β	pitch angle
σ_X	standard deviation of a variable X
Σ	a model system or a subsystem, e.g. a wind turbine
Σ_{FB}	feedback controller
Σ_{DC}	disturbance compensation
τ	prediction time of a signal
Ω_{rated}	rated rotor speed

References

Boukhezzar B. and Siguerdidjane H. (2005) Nonlinear control of variable speed wind turbines without wind speed measurement. *Proc. of the 44th IEEE Conf. on Decision and Control and the European Control Conf.*, Seville

Catch the Wind (2009) Boosting power production. Catch the Wind, Inc. **1**:15 pp

IEC (2005) IEC 61400-12-1 Wind turbines - Design requirements. Int. Electrotechnical Commission

Jonkman B. J. (2009) TurbSim User's Guide. Technical Report NREL/TP-500-46198, **1.5**, 85 pp

Jonkman B. J., Butterfield S., Musial W., and Scott G. (2009) Definition of a 5-MW reference wind turbine for offshore system development. Technical Report NREL/TP-500-38060, **1**, 75 pp

Schlipf D. and Kühn M. (2008) Prospects of a collective pitch control by means of predictive disturbance compensation assisted by wind speed measurements. *DEWEC* **1**:4 pp

Selvam K., Kane S., van Wingerden J. W., van Engelen T., and Verhaegen M. (2009) Feedback-feedforward individual pitch control for wind turbine load reduction. *Int. J. Robust Nonlinear Control* **19**:72–91